Analytic structure and power series expansion of the Jost function for the two-dimensional problem

2012 J. Phys. A: Math. Theor. 45 135209

(http://iopscience.iop.org/1751-8121/45/13/135209)

IOP Publishing Journal of Physics A: Mathematical and Theoretical

J. Phys. A: Math. Theor. **45** (2012) 135209 (28pp) doi:10.1088/1751-8113/45/13/135209

Analytic structure and power series expansion of the Jost function for the two-dimensional problem

S A Rakityansky[1] **and N Elander**[2]

[1] Department of Physics, University of Pretoria, Pretoria 0002, South Africa
[2] Division of Molecular Physics, Department of Physics, Stockholm University, Stockholm SE-106 91, Sweden

E-mail: rakitsa@up.ac.za

Received 30 December 2011, in final form 13 February 2012
Published 20 March 2012
Online at stacks.iop.org/JPhysA/45/135209

Abstract

For a two-dimensional quantum-mechanical problem, we obtain a generalized power series expansion of the *S*-matrix that can be done near an arbitrary point on the Riemann surface of the energy, similar to the standard effective-range expansion. In order to do this, we consider the Jost function and analytically factorize its momentum dependence that causes the Jost function to be a multi-valued function. The remaining single-valued function of the energy is then expanded in the power series near an arbitrary point in the complex energy plane. A systematic and accurate procedure has been developed for calculating the expansion coefficients. This makes it possible to obtain a semi-analytic expression for the Jost function (and therefore for the *S*-matrix) near an arbitrary point on the Riemann surface and use it, for example, to locate the spectral points (bound and resonant states) as the *S*-matrix poles. The method is applied to a model similar to those used in the theory of quantum dots.

PACS numbers: 03.65.Nk, 03.65.Ge, 24.30.Gd

1. Introduction

It is probable that an average reader of this journal perceives the one-dimensional (1D) and two-dimensional (2D) problems as simplified toy models of quantum mechanics. Although such an attitude has its roots in the standard courses of quantum mechanics, this perception is far from being adequate. First of all, modern nanotechnology allows us to fabricate microscopic quantum devices that behave and can be described as 1D or 2D. The 2D tunneling of particles plays an important role in superconductive tunnel junctions and even in some biological molecules [1]. Besides that, the corresponding quantum-mechanical problems are not mathematically simple as one may think. Indeed, in contrast to the motion of a particle in three-dimensional (3D) space, the 1D motion of the same particle on an infinite line is inherently a two-channel problem, where the channels are the left and right halves of the line

(see, for example, [2, 3]). As far as the 2D scattering is concerned, its amplitude as a function of the energy has not a square root but a logarithmic branching point (see [4–10] as well as the subsequent sections of this paper). Therefore from both pure mathematical and practical points of view, the 2D quantum problem is worthwhile to consider.

In this paper, we focus on solving the 2D problem with the help of power series that are similar to the famous effective-range expansion (where $\hbar k$ and δ_0 are the collision momentum and the S-wave phase shift)

$$k\cot\delta_0(k) = -\frac{1}{a} + \frac{1}{2}r_0k^2 - Pr_0^3k^4 + Qr_0^5k^6 + \cdots, \tag{1}$$

in terms of the so-called scattering length a, effective radius r_0, etc introduced long ago in nuclear physics [11].

As we already mentioned, the energy-dependent functions of the 2D problem have a logarithmic branching point at the threshold. As a result, there is a controversy concerning the 2D analogue of equation (1). Some authors [6–8, 12] define the scattering length a' by including it in the logarithmic term,

$$\cot\delta_0(k) = \frac{2}{\pi}\left(\gamma + \ln\frac{ka'}{2}\right) + \frac{r_0^2}{2\pi}k^2 + \mathcal{O}(k^4), \tag{2}$$

(here γ is Euler's constant), while others [4, 5] try to preserve the traditional form of the right-hand side of equation (1) and move the logarithmic term to the left-hand side:

$$\cot\delta_0(k) - \frac{2}{\pi}\left(\gamma + \ln\frac{k}{2}\right) = -\frac{2}{a''} + \mathcal{O}(k^2), \tag{3}$$

where $\ln a' = -\pi/a''$.

We look at this problem from a more general point of view. What is actually done in the original effective-range expansion (1) is the construction of the function $R(E) = k\cot\delta_0(k)$ in which the square-root branching of $k \sim \pm\sqrt{E}$ at the threshold is compensated by exactly the same branching of $\delta_0(k) \sim \pm\sqrt{E}$. As a result, the function $R(E)$ does not have branching points and is a single-valued analytic function of the energy $E \sim k^2$, and therefore can be expanded in a convergent series $R(E) = a_0 + a_1E + a_2E^2 + \cdots$, which is given by equation (1).

From this reasoning, a next logical step immediately follows: the function $R(E)$ can be expanded in a more general power series $R(E) = b_0 + b_1(E - E_0) + b_2(E - E_0)^2 + \cdots$ around an arbitrary complex energy E_0 within the domain of its analyticity. In [13, 14], we realized this idea for the 3D single-channel and multi-channel problems. In doing this, instead of using $R(E)$, we expanded the analytic single-valued parts of the Jost functions (or Jost matrices in the multi-channel case) after explicit separation of the factors that are responsible for the branching.

In this paper, we use the same approach as in [13, 14] to obtain similar expansions of the Jost functions for the 2D problem. First, we analyze the analytic structure of the Jost functions and split them into the single-valued and logarithmically branching parts. Then, we derive a set of differential equations that determine the single-valued parts. And finally, we look for the solutions of these equations in the form of power series of the energy. The series (2) and (3) together with simple recipes for calculating any number of their expansion coefficients are easily obtained from our more general expansions that are done around an arbitrary complex point E_0. Using the 2D model potential related to quantum dot theory, we numerically demonstrate the efficiency and accuracy of the proposed method.

2. Jost function

Radial part u_ℓ of the wavefunction describing the motion of a particle of mass μ with the energy E in a circularly symmetric 2D potential $U(r) = \hbar^2 V(r)/2\mu$ obeys the differential equation (a review of the partial-wave analysis for the 2D scattering is given in appendix A)

$$\left[\frac{\mathrm{d}^2}{\mathrm{d}r^2} + k^2 - \frac{\lambda(\lambda+1)}{r^2} - V(r)\right] u_\ell(E, r) = 0, \tag{4}$$

where $\ell = \lambda + 1/2$ is the angular momentum and $\lambda = -1/2, 1/2, 3/2, \ldots$. To avoid some mathematical complications, we assume that the potential $V(r)$ is of short range, i.e. it vanishes at large distances faster than any power of $1/r$ (for example, exponentially). Then at large distances, where $V(r) \to 0$, the radial equation simplifies

$$\left[\frac{\mathrm{d}^2}{\mathrm{d}r^2} + k^2 - \frac{\lambda(\lambda+1)}{r^2}\right] u_\ell(E, r) \approx 0, \qquad r \to \infty. \tag{5}$$

This is the Riccati–Bessel equation. As its two linearly independent solutions, we can choose either the Riccati–Bessel and Riccati–Neumann functions $j_\lambda(kr)$ and $y_\lambda(kr)$, or the two Riccati–Hankel functions $h_\lambda^{(\pm)}(kr)$. Any other solution of equation (5) is a superposition of the two linearly independent solutions. In particular, we can write the asymptotics of the physical wavefunction as a linear combination of the Riccati–Hankel functions,

$$u_\ell(E, r) \underset{r\to\infty}{\longrightarrow} f_\ell^{(\mathrm{in})}(E) h_{\ell-1/2}^{(-)}(kr) + f_\ell^{(\mathrm{out})}(E) h_{\ell-1/2}^{(+)}(kr), \tag{6}$$

where the energy-dependent combination coefficients $f_\ell^{(\mathrm{in/out})}(E)$ are called the Jost functions. When $r \to \infty$, the Riccati–Hankel functions represent the incoming and outgoing circular waves. Indeed,

$$h_{\ell-1/2}^{(\pm)}(kr) = \sqrt{\frac{\pi kr}{2}} H_\ell^{(\pm)}(kr) \underset{|z|\to\infty}{\longrightarrow} \mathrm{e}^{\pm\mathrm{i}(kr - \ell\pi/2 - \pi/4)} = \mp\mathrm{i}\,\mathrm{e}^{\pm\mathrm{i}(kr - \lambda\pi/2)}, \tag{7}$$

where $H_\ell^{(\pm)}(z)$ are the cylindrical Hankel functions. The Jost functions $f_\ell^{(\mathrm{in/out})}(E)$ are therefore the asymptotic amplitudes of the incoming and outgoing waves. Since the flux of the particles is conserving, for real E we have $\left|f_\ell^{(\mathrm{in})}(E)\right| = \left|f_\ell^{(\mathrm{out})}(E)\right|$. Actually, these two functions are related to each other at different complex values of E as well. Some of such symmetry properties can be established using the semi-analytic structure of them that is derived in the subsequent sections. It can also be shown that the partial-wave S-matrix is the ratio of these functions

$$s_\ell(E) = \frac{f_\ell^{(\mathrm{out})}(E)}{f_\ell^{(\mathrm{in})}(E)}, \tag{8}$$

and that zeros of the Jost function $f_\ell^{(\mathrm{in})}(E)$ are the discrete spectral points $\mathcal{E}_n$,

$$f_\ell^{(\mathrm{in})}(\mathcal{E}_n) = 0, \tag{9}$$

i.e. the bound and resonant states of the system.

3. Transformation of the radial equation

Our goal is to establish the analytic structure of the Jost function, i.e. to find such an expression for it where all possible non-analytic dependences on the energy are given explicitly. This can be done if we transform the second-order radial equation (4) into an equivalent set of first-order equations.

The transformation is done using a method which is known in the theory of differential equations as the variation parameter method [15, 16]. Following this method, we look for the unknown function $u_\ell(E, r)$ in the form similar to its asymptotics (6), but with the combination coefficients being new unknown functions of r,

$$u_\ell(E, r) = F_\ell^{(\mathrm{in})}(E, r)h_{\ell-1/2}^{(-)}(kr) + F_\ell^{(\mathrm{out})}(E, r)h_{\ell-1/2}^{(+)}(kr), \tag{10}$$

where $F_\ell^{(\mathrm{in/out})}(E, r)$ are the new unknown functions. Since instead of one unknown function we introduce two of them, they cannot be independent of each other. In principle, we can impose any reasonable condition relating them. Looking at the asymptotics (6), we see that

$$f_\ell^{(\mathrm{in})}(E) = \lim_{r\to\infty} F_\ell^{(\mathrm{in})}(E, r), \qquad f_\ell^{(\mathrm{out})}(E) = \lim_{r\to\infty} F_\ell^{(\mathrm{out})}(E, r). \tag{11}$$

Therefore, at large distances our new functions become constants, and we should have

$$\big[\partial_r F_\ell^{(\mathrm{in})}\big]h_\lambda^{(-)}(kr) + \big[\partial_r F_\ell^{(\mathrm{out})}\big]h_\lambda^{(+)}(kr) = 0. \tag{12}$$

As the additional condition imposed on these functions, we demand that relation (12) is valid not only at large r but at all distances. In the variation parameter method, this condition is known as the Lagrange condition. In our case, this condition makes $F_\ell^{(\mathrm{in/out})}(E, r)$ to be the Jost functions for the potential which is cut-off at the radius r (in the spirit of the variable-phase approach).

Substituting the ansatz (10) into the radial equation (4) and using the Lagrange condition (12) together with the known Wronskian of the Riccati–Hankel functions,

$$h_\lambda^{(-)}(kr)\partial_r h_\lambda^{(+)}(kr) - h_\lambda^{(+)}(kr)\partial_r h_\lambda^{(-)}(kr) = 2\mathrm{i}k, \tag{13}$$

we obtain a set of two first-order equations which are equivalent to the original radial equation (4),

$$\partial_r F_\ell^{(\mathrm{in})} = -\frac{1}{2\mathrm{i}k}h_\lambda^{(+)}V\big[F_\ell^{(\mathrm{in})}h_\lambda^{(-)} + F_\ell^{(\mathrm{out})}h_\lambda^{(+)}\big], \tag{14}$$

$$\partial_r F_\ell^{(\mathrm{out})} = +\frac{1}{2\mathrm{i}k}h_\lambda^{(-)}V\big[F_\ell^{(\mathrm{in})}h_\lambda^{(-)} + F_\ell^{(\mathrm{out})}h_\lambda^{(+)}\big]. \tag{15}$$

The boundary conditions for these equations follow from the requirement that the wavefunction must be regular everywhere. In particular, this means that $u_\ell(E, 0) = 0$. It seems that this is not the case because both $h_\lambda^{(+)}(kr)$ and $h_\lambda^{(-)}(kr)$ that are present in expression (10) are singular at $r = 0$. Their singularities, however, can cancel each other,

$$h_\lambda^{(+)}(z) + h_\lambda^{(-)}(z) = 2j_\lambda(z), \tag{16}$$

if they are superimposed with the same coefficient. This can be achieved if both $F_\ell^{(\mathrm{in})}(E, r)$ and $F_\ell^{(\mathrm{out})}(E, r)$ have the same value at $r = 0$,

$$F_\ell^{(\mathrm{in})}(E, 0) = F_\ell^{(\mathrm{out})}(E, 0).$$

Their common value at $r = 0$ determines the overall normalization of the wavefunction and therefore can be chosen arbitrarily. To be consistent, we chose it to be 1/2, which makes $u_\ell(E, r)$ behave near the origin exactly as the Riccati–Bessel function and thus the solution with the boundary conditions

$$F_\ell^{(\mathrm{in})}(E, 0) = F_\ell^{(\mathrm{out})}(E, 0) = \tfrac{1}{2} \tag{17}$$

is what is called the regular solution in the theory of 3D scattering.

For our goal of expressing the non-analytic dependences of the Jost functions in an explicit form, it is more convenient to re-write the ansatz (10) in terms of the Riccati–Bessel and Riccati–Neumann functions

$$u_\ell(E, r) = A_\ell(E, r)\, j_\lambda(kr) - B_\ell(E, r)y_\lambda(kr), \tag{18}$$

and to obtain the corresponding equations for the unknown functions $A_\ell(E, r)$ and $B_\ell(E, r)$. Since

$$h_\lambda^{(\pm)}(z) = j_\lambda(z) \pm \mathrm{i} y_\lambda(z), \tag{19}$$

this is most simply achieved by making the following linear combinations of equations (14) and (15):

$$A_\ell(E, r) = F_\ell^{(\mathrm{in})}(E, r) + F_\ell^{(\mathrm{out})}(E, r), \tag{20}$$

$$B_\ell(E, r) = \mathrm{i}\big[F_\ell^{(\mathrm{in})}(E, r) - F_\ell^{(\mathrm{out})}(E, r)\big]. \tag{21}$$

This gives

$$\partial_r A_\ell = -\frac{1}{k} y_\lambda V (A_\ell j_\lambda - B_\ell y_\lambda), \tag{22}$$

$$\partial_r B_\ell = -\frac{1}{k} j_\lambda V (A_\ell j_\lambda - B_\ell y_\lambda) \tag{23}$$

with the boundary conditions

$$A_\ell(E, 0) = 1, \qquad B_\ell(E, 0) = 0. \tag{24}$$

4. Complex rotation

Suppose that the potential $V(r)$ is cut off at certain radius $r = R$, then the right-hand sides of the sets of equations (14), (15) or (22), (23) vanish at $r > R$ and thus the derivatives on the left-hand sides of these equations become zero, i.e. the functions $F_\ell^{(\mathrm{in/out})}$ or A_ℓ and B_ℓ do not change beyond this point. Therefore, in the spirit of the variable-phase approach, the functions $F_\ell^{(\mathrm{in/out})}(E, r)$ are the Jost functions for the potential which is cut off at the point r. Generally speaking, when the potential asymptotically vanishes at large distances, we should expect the convergence of the limits (11).

Therefore, the Jost functions can be calculated by numerical integration of the differential equations (14), (15) or (22), (23) from $r = 0$ up to a sufficiently large radius R where the limits (11) are reached within a required accuracy. This works perfectly for real values of the energy E. However, when we consider complex energies (for example, in search for resonances), a technical difficulty arises. This difficulty is caused by the asymptotic behavior (7) of the Riccati–Hankel functions.

When k is complex, either $h_\lambda^{(+)}(kr)$ or $h_\lambda^{(-)}(kr)$ exponentially diverges, depending on the sign of $\mathrm{Im}\, k$. As a result, either equation (14) or equation (15) does not give a numerically convergent solution. This difficulty is circumvented by using the deformed integration path shown in figure 1. Instead of integrating the differential equations along the real axis from $r = 0$ to $r = R$, we can reach the final point via the intermediate point $r = R'$ in the complex plane. Moreover, we can safely ignore the arc $R'R$ since the potential is practically zero at that distance.

Such a complex rotation helps because the asymptotic behavior (divergent or convergent) of the functions $h_\lambda^{(\pm)}(kr)$ is determined by the sign of $\mathrm{Im}\, kr$. For a given $k = |k|\, \mathrm{e}^{\mathrm{i}\phi}$, we can always find such a rotation angle θ in $r = |r|\, \mathrm{e}^{-\mathrm{i}\theta}$ that the product $kr = |kr|\mathrm{e}^{\mathrm{i}(\phi-\theta)}$ has either positive or negative (or even zero) imaginary part. Various technical details of using complex rotation in calculating the Jost functions and Jost matrices can be found in [2, 3, 13, 14, 18–25].

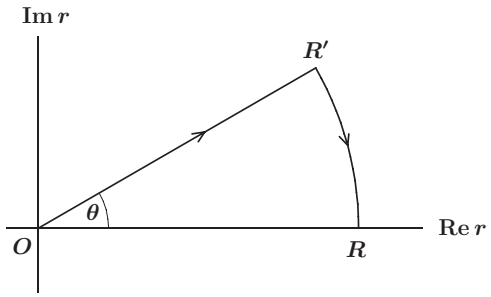

Figure 1. Deformed contour for integrating differential equations (14) and (15), and (22) and (23).

5. Explicit separation of the non-analytic factors

In order to establish the analytic structure of the Jost functions, we need to have a closer look at the structure of the Riccati–Bessel and Riccati–Neumann functions. The following expressions for them (they can be derived using formulae (9.1.2), (9.1.10) and (9.1.11) of [17]) are the most useful for this

$$j_\lambda(kr) = k^{\lambda+1}\sum_{n=0}^{\infty} k^{2n} f_n^{(\lambda)}(r), \tag{25}$$

$$y_\lambda(kr) = k^{-\lambda}\sum_{n=0}^{\infty} k^{2n} g_n^{(\lambda)}(r) + h(k)\, j_\lambda(kr), \tag{26}$$

where

$$f_n^{(\lambda)}(r) = \frac{\sqrt{\pi}(-1)^n}{n!\Gamma(n+\lambda+3/2)}\left(\frac{r}{2}\right)^{2n+\lambda+1}, \qquad \text{for any } \lambda. \tag{27}$$

If λ is an integer, then the expansion of $y_\lambda(kr)$ is also simple:

$$g_n^{(\lambda)}(r) = \frac{\sqrt{\pi}(-1)^{n+\lambda+1}}{n!\Gamma(n-\lambda+1/2)}\left(\frac{r}{2}\right)^{2n-\lambda}, \tag{28}$$

$$h(k) = 0. \tag{29}$$

However, for a half-integer λ, we have a more difficult case

$$g_n^{(\lambda)}(r) = \begin{cases} -\dfrac{(\lambda-n-1/2)!}{\sqrt{\pi}n!}\left(\dfrac{r}{2}\right)^{2n-\lambda}, & 0 \leqslant n \leqslant \lambda - \frac{1}{2}, \\ \dfrac{2}{\pi}\ln\left(\dfrac{r}{R}\right) f^{(\lambda)}_{n-\lambda-\frac{1}{2}}(r) & \\ -\dfrac{(-1)^{n-\lambda-\frac{1}{2}}\left[\psi(n+1)+\psi(n-\lambda+\frac{1}{2})\right]}{\sqrt{\pi}n!(n-\lambda-\frac{1}{2})!}\left(\dfrac{r}{2}\right)^{2n-\lambda}, & \lambda+\frac{1}{2} \leqslant n < \infty, \end{cases} \tag{30}$$

$$h(k) = \frac{2}{\pi}\ln\left(\frac{kR}{2}\right), \tag{31}$$

where R is an arbitrary number (in the units of length). It is arbitrary because any increase or decrease of $h(k)$ caused by the change of R is compensated by the corresponding change in the first term of equation (30). The parameter R is introduced to separate the r and k dependences

in the original term containing $\ln(kr/2) = \ln(kR/2) + \ln(r/R)$ and to have dimensionless products under the logarithm. In practical calculations the parameter R can always be taken as the unit of the length, i.e. $R = 1$. The ψ-function in equation (30) is defined as follows [17]:

$$\psi(n) = \frac{\Gamma'(n)}{\Gamma(n)} = \begin{cases} -\gamma, & n = 1, \\ -\gamma + \sum_{m=1}^{n-1} m^{-1}, & n \geqslant 2, \end{cases} \tag{32}$$

where $\gamma = 0.577\ldots$ is the Euler constant.

Equations (25) and (26) represent the Riccati–Bessel and Riccati–Neumann functions in the form of infinite series. Each term of these series is a product of a function depending on k and another function depending on r, i.e. the k and r dependences are given in a separable form.

What do the above formulae tell us about the Jost functions? The functions $j_\lambda(kr)$ and $y_\lambda(kr)$ are involved in the coefficients of the differential equations (22) and (23) that determine the Jost functions. This means that the Jost functions are not single-valued functions of the energy. Indeed, for each choice of E, we have two possible values of the momentum

$$k = \pm\sqrt{\frac{2\mu E}{\hbar^2}}.$$

The index $\lambda = -1/2,\ 1/2,\ 3/2, \ldots$ of the Riccati functions is a half-integer. This means that the differential equations involve square root and logarithm of the momentum.

Therefore, the Jost functions are defined on a complicated Riemann surface and the threshold point $E = 0$ is a branching point of this surface. It would be desirable to find an expression for the Jost functions in terms of the powers of $\sqrt{k}$, the logarithmic function $h(k)$ and some entire single-valued functions of E. In order to do this, we note that the series in equations (25) and (26) involve only even powers of k, i.e. the powers of the energy $k^2 = 2\mu E/\hbar^2$. Since for any finite r these series are absolutely and uniformly convergent on the whole complex plane of E, they define some entire functions, i.e.

$$j_\lambda(kr) = k^{\lambda+1}\tilde{j}_\lambda(E, r), \tag{33}$$

$$y_\lambda(kr) = k^{-\lambda}\tilde{y}_\lambda(E, r) + k^{\lambda+1}h(k)\tilde{j}_\lambda(E, r), \tag{34}$$

where the 'tilded' functions

$$\tilde{j}_\lambda(E, r) = \sum_{n=0}^{\infty}\left(\frac{2\mu E}{\hbar^2}\right)^n f_n^{(\lambda)}(r), \tag{35}$$

$$\tilde{y}_\lambda(E, r) = \sum_{n=0}^{\infty}\left(\frac{2\mu E}{\hbar^2}\right)^n g_n^{(\lambda)}(r), \tag{36}$$

are single-valued entire functions of complex variable E.

Let us find a similar structure for the functions $A_\ell(E, r)$ and $B_\ell(E, r)$ and through them for $F_\ell^{(\text{in/out})}(E, r)$. For this, we replace the set of equations (22) and (23) with their linear combinations, namely we multiply equation (23) by $h(k)$ and subtract the result from equation (22), and as the second equation, we take equation (23) multiplied by $k^{-(2\lambda+1)}$. As a result, we obtain

$$\partial_r(A_\ell - hB_\ell) = -\frac{1}{k}(y_\lambda - hj_\lambda)V(A_\ell j_\lambda - B_\ell y_\lambda), \tag{37}$$

$$\partial_r k^{-(2\lambda+1)}B_\ell = -k^{-2(\lambda+1)}j_\lambda V(A_\ell j_\lambda - B_\ell y_\lambda). \tag{38}$$

Now, taking into account equations (33) and (34), we see that

$$y_\lambda - hj_\lambda = k^{-\lambda}\tilde{y}_\lambda + k^{\lambda+1}h\tilde{j}_\lambda - k^{\lambda+1}h\tilde{j}_\lambda = k^{-\lambda}\tilde{y}_\lambda$$

and

$$\begin{aligned} A_\ell j_\lambda - B_\ell y_\lambda &= A_\ell k^{\lambda+1}\tilde{j}_\lambda - B_\ell k^{-\lambda}\tilde{y}_\lambda - B_\ell k^{\lambda+1}h\tilde{j}_\lambda \\ &= k^{\lambda+1}(A_\ell - hB_\ell)\tilde{j}_\lambda - k^{-\lambda}B_\ell\tilde{y}_\lambda. \end{aligned}$$

Substituting these expressions into equations (37) and (38), we have

$$\partial_r(A_\ell - hB_\ell) = -k^{-(\lambda+1)}\tilde{y}_\lambda V[k^{\lambda+1}(A_\ell - hB_\ell)\tilde{j}_\lambda - k^{-\lambda}B_\ell\tilde{y}_\lambda], \tag{39}$$

$$\partial_r k^{-(2\lambda+1)}B_\ell = -k^{-(\lambda+1)}\tilde{j}_\lambda V[k^{\lambda+1}(A_\ell - hB_\ell)\tilde{j}_\lambda - k^{-\lambda}B_\ell\tilde{y}_\lambda]. \tag{40}$$

If we introduce the 'tilded' functions

$$\tilde{A}_\ell(E,r) \equiv A_\ell(E,r) - h(k)B_\ell(E,k), \tag{41}$$

$$\tilde{B}_\ell(E,r) \equiv k^{-(2\lambda+1)}B_\ell(E,r), \tag{42}$$

then equations (39) and (40) assume the following form:

$$\partial_r\tilde{A}_\ell = -\tilde{y}_\lambda V(\tilde{A}_\ell\tilde{j}_\lambda - \tilde{B}_\ell\tilde{y}_\lambda), \tag{43}$$

$$\partial_r\tilde{B}_\ell = -\tilde{j}_\lambda V(\tilde{A}_\ell\tilde{j}_\lambda - \tilde{B}_\ell\tilde{y}_\lambda) \tag{44}$$

with the boundary conditions (that follow from (24))

$$\tilde{A}_\ell(E,0) = 1, \qquad \tilde{B}_\ell(E,0) = 0. \tag{45}$$

For any finite r, all the coefficient functions in equations (43) and (44) are entire functions of the parameter E and the boundary conditions are E-independent. According to the Poincaré theorem [26] the solutions of these equations, i.e. the functions $\tilde{A}_\ell(E,r)$ and $\tilde{B}_\ell(E,r)$, are entire (analytic single-valued) functions of the complex variable E.

Therefore the structure we wanted to find is as follows:

$$A_\ell(E,r) = \tilde{A}_\ell(E,r) + k^{2\lambda+1}h(k)\tilde{B}_\ell(E,r), \tag{46}$$

$$B_\ell(E,r) = k^{2\lambda+1}\tilde{B}_\ell(E,r), \tag{47}$$

where $\tilde{A}_\ell(E,r)$ and $\tilde{B}_\ell(E,r)$ are single-valued analytic functions of E. Apart from these single-valued functions, the original functions A_ℓ and B_ℓ involve the factors $k^{2\lambda+1}$ and $h(k)$. Since λ is a half-integer, the power $(2\lambda+1)$ is always even and thus $k^{2\lambda+1}$ is also a single-valued function of E, but $h(k)$ has a logarithmic branching point at $E = 0$.

The functions $F_\ell^{(\mathrm{in/out})}$ have a similar structure

$$F_\ell^{(\mathrm{in})}(E,r) = \tfrac{1}{2}(A_\ell - \mathrm{i}B_\ell) = \tfrac{1}{2}\{\tilde{A}_\ell(E,r) + k^{2\lambda+1}[h(k) - \mathrm{i}]\tilde{B}_\ell(E,r)\}, \tag{48}$$

$$F_\ell^{(\mathrm{out})}(E,r) = \tfrac{1}{2}(A_\ell + \mathrm{i}B_\ell) = \tfrac{1}{2}\{\tilde{A}_\ell(E,r) + k^{2\lambda+1}[h(k) + \mathrm{i}]\tilde{B}_\ell(E,r)\}. \tag{49}$$

6. Analytic structure of the Jost functions

What we have established in the previous section is valid for any complex E and any finite distance r. In other words, so far we have established that the Jost functions (11) have the structure (48), (49) if the potential is cut off at a certain radius $r = R$ (does not matter how large R is). The problem is that to prove the analyticity of $\tilde{A}_\ell(E, r)$ and $\tilde{B}_\ell(E, r)$ with respect to the variable E, we used the Poincaré theorem which requires that the coefficients of equations (43) and (44) be holomorphic functions of E. If E is a real positive number and the potential is of short range, this is true even if $r \to \infty$. Indeed, in such a case both $\tilde{j}_\lambda(kr)$ and $\tilde{y}_\lambda(kr)$ oscillate with finite amplitudes even at infinity and thus the coefficients of equations (43) and (44) simply tend to zero (i.e. remain holomorphic) when $r \to \infty$. If however E is negative or complex, then generally speaking this is not true. As we will see shortly, there is still a domain of complex E where the coefficients remain holomorphic. In other words, if we extend r to infinity, we have to narrow the domain of E.

The Riccati–Bessel and Riccati–Neumann functions are linear combinations of the Riccati–Hankel functions and thus at large distances behave as exponential functions (7). If the momentum has a nonzero imaginary part, then one or the other of these exponentials is diverging and thus both $\tilde{j}_\lambda(kr)$ and $\tilde{y}_\lambda(kr)$ tend to infinity when $r \to \infty$. To some extent, the situation can be saved by using a short-range (exponentially decaying) potential $V(r) \sim \exp(-\eta r)$, which compensates the divergence of $\tilde{j}_\lambda(kr)$ and $\tilde{y}_\lambda(kr)$ within a certain domain $\mathcal{D}$ of the complex E-plane along its real axis. The borders of the domain $\mathcal{D}$ are determined by the requirement that none of the coefficients of equations (43) and (44) are divergent. The behavior (convergent or divergent) of these coefficients is determined by the product $\exp(\pm 2ikr)\exp(-\eta r)$. For a given η it is not difficult to find the domain $\mathcal{D}$,

$$\mathcal{D} = \{E : |2\,\mathrm{Im}\sqrt{2\mu E/\hbar^2}| < \eta\}, \tag{50}$$

which gives the condition

$$(\mathrm{Im}\,E)^2 < \frac{\hbar^4\eta^4}{16\mu^2} + \frac{\hbar^2\eta^2}{2\mu}\,\mathrm{Re}\,E. \tag{51}$$

A similar analyticity domain was obtained by Motovilov [27] for the 3D multi-channel T-matrix, using a rigorous analysis of the corresponding scattering operators.

The faster the potential decays, the wider is the domain. An example of such a domain is shown in figure 2 for the model used in section 9. It is a parabolic domain along the real axis, whose border is shown by the solid curve. It crosses the real axis at $E \approx -0.0332$ (in donor Hartree units). When $r \to \infty$, we can only use the Poincaré theorem within $\mathcal{D}$, and thus we can say that at least within this domain, the functions $\tilde{A}_\ell(E, \infty)$ and $\tilde{B}_\ell(E, \infty)$ are the holomorphic functions of variable E.

If the potential $V(r)$ (or at least its long-range tail) is an analytic function of a complex variable r and exponentially decays along any ray $r = |r|e^{i\theta}$ within a certain sector of the complex r-plane, then the domain $\mathcal{D}$ can be extended by using the complex rotation described in section 4. With a complex radius, the product $\exp(\pm 2ikr)\exp(-\eta r)$ vanishes at infinity if E is within

$$\mathcal{D} = \{E : |2\,\mathrm{Im}\,(kr)| < \eta\,\mathrm{Re}\,r\}, \tag{52}$$

which generalizes equation (50). It is easy to show that if $E = |E|\exp(i\chi)$, then such a domain can be defined by the following inequality:

$$\sin^2\left(\frac{\chi}{2} + \theta\right) < \frac{\hbar^2\eta^2\cos^2\theta}{8\mu|E|}. \tag{53}$$

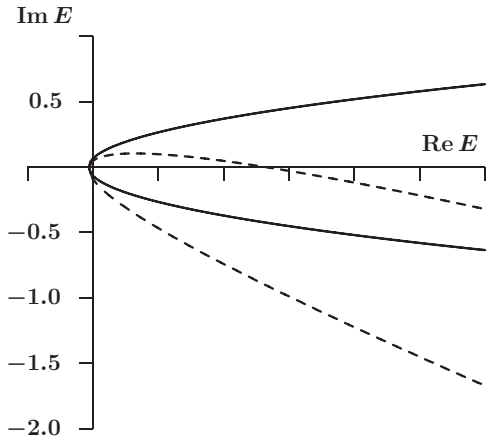

Figure 2. Domains $\mathcal{D}$ for the potential (84), defined by equation (51) (within the solid curve) and by equation (53) for the rotation angle $\theta = 0.05\pi$ (within the dashed curve). The energy is given in the donor Hartree units (see section 9).

With $\theta = 0$, this condition is transformed into (51). An example of such a domain with the rotation angle $\theta = 0.05\pi$ for the potential (84) is shown by the dashed curve in figure 2.

The physically interesting domain of the E-plane where the structure (48), (49) can be used in practical calculations, lies on the positive real axis (scattering) and in the close vicinity below it (pronounced resonances). Therefore, we can say that for all practical purposes, this structure is valid at an arbitrary point E.

If we denote the asymptotic values (within $\mathcal{D}$) of the 'tilded' functions as

$$\tilde{a}_\ell(E) = \lim_{r\to\infty} \tilde{A}_\ell(E, r), \qquad \tilde{b}_\ell(E) = \lim_{r\to\infty} \tilde{B}_\ell(E, r), \tag{54}$$

then the Jost functions and the S-matrix can be written as follows:

$$f_\ell^{(\mathrm{in})}(E) = \frac{1}{2}\{\tilde{a}_\ell(E) + k^{2\lambda+1}[h(k) - \mathrm{i}]\tilde{b}_\ell(E)\}, \tag{55}$$

$$f_\ell^{(\mathrm{out})}(E) = \frac{1}{2}\{\tilde{a}_\ell(E) + k^{2\lambda+1}[h(k) + \mathrm{i}]\tilde{b}_\ell(E)\}, \tag{56}$$

$$s_\ell(E) = \frac{\tilde{a}_\ell(E) + k^{2\lambda+1}[h(k) + \mathrm{i}]\tilde{b}_\ell(E)}{\tilde{a}_\ell(E) + k^{2\lambda+1}[h(k) - \mathrm{i}]\tilde{b}_\ell(E)}. \tag{57}$$

To find the Jost functions or the S-matrix on any sheet of the Riemann surface, we need to calculate the functions $\tilde{a}_\ell(E)$ and $\tilde{b}_\ell(E)$ only once (because they are single valued). The choice of the sheet is determined by an appropriate choice of the value of the logarithmic function $h(k)$. Please note that $k^{2\lambda+1} = k^{2\ell}$ is a single-valued function of E.

7. Power series expansions of the Jost functions

The functions $\tilde{a}_\ell(E)$ and $\tilde{b}_\ell(E)$ are holomorphic (i.e. single valued and analytic) and therefore can be expanded in the Taylor series near any point E_0 within the domain $\mathcal{D}$ of the complex energy plane. The expansion around the point $E_0 = 0$ will give us the standard effective-range

series. But we can also do such an expansion near an arbitrary point

$$\tilde{a}_\ell(E) = \sum_{n=0}^{\infty} \alpha_n^{(\ell)}(E_0)(E - E_0)^n, \tag{58}$$

$$\tilde{b}_\ell(E) = \sum_{n=0}^{\infty} \beta_n^{(\ell)}(E_0)(E - E_0)^n. \tag{59}$$

How can the expansion coefficients $\alpha_n^{(\ell)}$ and $\beta_n^{(\ell)}$ be found? For this purpose, we can derive differential equations, the solutions of which asymptotically tend to $\alpha_n^{(\ell)}$ and $\beta_n^{(\ell)}$. Indeed, such an expansion can be done at any fixed radius r because the functions $\tilde{A}_\ell(E, r)$ and $\tilde{B}_\ell(E, r)$ reach their limits (54) at r if the potential is cut off at this radius (in the spirit of the variable-phase approach). Therefore for each r, we have

$$\tilde{A}_\ell(E, r) = \sum_{n=0}^{\infty} \mathcal{A}_n^{(\ell)}(E_0, r)(E - E_0)^n, \tag{60}$$

$$\tilde{B}_\ell(E, r) = \sum_{n=0}^{\infty} \mathcal{B}_n^{(\ell)}(E_0, r)(E - E_0)^n, \tag{61}$$

where

$$\alpha_n^{(\ell)}(E_0) = \lim_{r\to\infty} \mathcal{A}_n^{(\ell)}(E_0, r), \qquad \beta_n^{(\ell)}(E_0) = \lim_{r\to\infty} \mathcal{B}_n^{(\ell)}(E_0, r). \tag{62}$$

Therefore, the differential equations mentioned above should determine the functions $\mathcal{A}_n^{(\ell)}(E_0, r)$ and $\mathcal{B}_n^{(\ell)}(E_0, r)$. In order to obtain such equations, we expand the 'tilded' functions $\tilde{j}_\lambda(E, r)$ and $\tilde{y}_\lambda(E, r)$ in the Taylor series near an arbitrary point E_0

$$\tilde{j}_\lambda(E, r) = \sum_{n=0}^{\infty} s_n^{(\lambda)}(E_0, r)\,(E - E_0)^n\,, \tag{63}$$

$$\tilde{y}_\lambda(E, r) = \sum_{n=0}^{\infty} c_n^{(\lambda)}(E_0, r)\,(E - E_0)^n\,, \tag{64}$$

which are more general expansions than the series (35), (36) for the particular case of the threshold energy $E_0 = 0$. Any number of the expansion coefficients $s_n^{(\lambda)}(E_0, r)$ and $c_n^{(\lambda)}(E_0, r)$ can be found using the recurrence relations derived in appendix B.

Substituting expansions (60), (61), (63) and (64) into equations (43) and (44), and equalizing the factors of the same powers of $(E - E_0)$, we obtain the equations we are looking for,

$$\partial_r \tilde{\mathcal{A}}_n^{(\ell)} = -\sum_{i+j+k=n} c_i^{(\lambda)} V\big(\tilde{\mathcal{A}}_j^{(\ell)} s_k^{(\lambda)} - \tilde{\mathcal{B}}_j^{(\ell)} c_k^{(\lambda)}\big), \tag{65}$$

$$\partial_r \tilde{\mathcal{B}}_n^{(\ell)} = -\sum_{i+j+k=n} s_i^{(\lambda)} V\big(\tilde{\mathcal{A}}_j^{(\ell)} s_k^{(\lambda)} - \tilde{\mathcal{B}}_j^{(\ell)} c_k^{(\lambda)}\big), \tag{66}$$

with the boundary conditions

$$\tilde{\mathcal{A}}_n^{(\ell)}(E_0, 0) = \delta_{n0}, \qquad \tilde{\mathcal{B}}_n^{(\ell)}(E_0, 0) = 0, \qquad n = 0, 1, 2, 3, \ldots. \tag{67}$$

These conditions follow from the fact that the corresponding boundary conditions (45) do not depend on E. Therefore, starting with the initial values (67) at $r = 0$, and numerically solving

the first $N+1$ pairs of differential equations of the system (65), (66) up to a sufficiently large radius $r_{\max}$, we obtain the first $N+1$ expansion coefficients:

$$\alpha_n^{(\ell)}(E_0) = \tilde{\mathcal{A}}_n^{(\ell)}(E_0, r_{\max}), \qquad \beta_n^{(\ell)}(E_0) = \tilde{\mathcal{B}}_n^{(\ell)}(E_0, r_{\max}), \qquad n = 0, 1, 2, \ldots, N. \tag{68}$$

These coefficients give us the following approximate formulae for the Jost functions:

$$f_\ell^{(\mathrm{in})}(E) \approx \frac{1}{2}\sum_{n=0}^{N}\left\{\alpha_n^{(\ell)}(E_0) + k^{2\lambda+1}[h(k) - \mathrm{i}]\beta_n^{(\ell)}(E_0)\right\}(E - E_0)^n, \tag{69}$$

$$f_\ell^{(\mathrm{out})}(E) \approx \frac{1}{2}\sum_{n=0}^{N}\left\{\alpha_n^{(\ell)}(E_0) + k^{2\lambda+1}[h(k) + \mathrm{i}]\beta_n^{(\ell)}(E_0)\right\}(E - E_0)^n, \tag{70}$$

which are valid for any complex value of E within a domain around the chosen central point E_0. Apparently, the closer the E to E_0, the better the accuracy of these formulae. It is interesting to note that equation (9) of [10] is the first term of equation (69) for the particular case of $E_0 = 0$.

An alternative way of using formulae (69) and (70) is to treat the expansion coefficients $\alpha_n^{(\ell)}(E_0)$, $\beta_n^{(\ell)}(E_0)$, $n = 0, 1, \ldots, N$ as fitting parameters. Adjusting them in such a way that the corresponding cross section (see appendix A4) reproduces experimental data in the vicinity of a real energy E_0, one then can use the Jost function (69) at the nearby complex energies for locating possible resonances. The obvious advantage of such an approach is that the resonance energy and the width are deduced directly from experimental data using correct analytic structure of the S-matrix.

8. Effective-range expansion

Far away from the interaction region, the radial wavefunction (18) is a linear combination of the Riccati–Bessel and Riccati–Neumann functions

$$u_\ell(E, r) \underset{r\to\infty}{\longrightarrow} a_\ell(E) j_\lambda(kr) - b_\ell(E) y_\lambda(kr), \tag{71}$$

where

$$a_\ell(E) = \lim_{r\to\infty} A_\ell(E, r), \qquad b_\ell(E) = \lim_{r\to\infty} B_\ell(E, r). \tag{72}$$

The functions j_λ and y_λ in (71) can be written in their asymptotic form

$$j_\lambda(kr) \underset{r\to\infty}{\longrightarrow} \sin\left(kr - \frac{\lambda\pi}{2}\right), \tag{73}$$

$$y_\lambda(kr) \underset{r\to\infty}{\longrightarrow} -\cos\left(kr - \frac{\lambda\pi}{2}\right), \tag{74}$$

which gives

$$u_\ell(E, r) \underset{r\to\infty}{\longrightarrow} a_\ell(E)\sin\left(kr - \frac{\lambda\pi}{2}\right) + b_\ell(E)\cos\left(kr - \frac{\lambda\pi}{2}\right)$$

$$= N\sin\left[kr - \frac{\lambda\pi}{2} + \delta_\ell(E)\right],$$

where a_ℓ and b_ℓ are replaced with their common normalization factor N and the scattering phase shift δ_ℓ,

$$a_\ell(E) = N\cos\delta_\ell(E), \tag{75}$$

$$b_\ell(E) = N \sin \delta_\ell(E). \tag{76}$$

Using relations (46) and (47) at large distances ($r \to \infty$),

$$a_\ell(E) = \tilde{a}_\ell(E) + k^{2\lambda+1} h(k) \tilde{b}_\ell(E), \tag{77}$$

$$b_\ell(E) = k^{2\lambda+1} \tilde{b}_\ell(E), \tag{78}$$

we can construct the so-called effective-range function which is a holomorphic function of the energy. This is done by taking the ratio

$$\cot \delta_\ell = \frac{a_\ell}{b_\ell} = \frac{\tilde{a}_\ell + k^{2\lambda+1} h \tilde{b}_\ell}{k^{2\lambda+1} \tilde{b}_\ell},$$

and moving all the 'troublesome' terms and factors, which may generate singularities, to the left-hand side of the equation

$$k^{2\lambda+1} \cot \delta_\ell = \frac{\tilde{a}_\ell}{\tilde{b}_\ell} + k^{2\lambda+1} h,$$

$$k^{2\lambda+1} \left[\cot \delta_\ell(E) - h(k)\right] = k^{2\ell} \left[\cot \delta_\ell(E) - h(k)\right] = \frac{\tilde{a}_\ell(E)}{\tilde{b}_\ell(E)}. \tag{79}$$

Both the numerator and denominator in the last ratio can be written in the form of power series (58), (59) with $E_0 = 0$

$$k^{2\lambda+1} \left[\cot \delta_\ell(E) - h(k)\right] = \frac{\sum_{n=0}^{\infty} \alpha_n^{(\ell)}(0) E^n}{\sum_{n=0}^{\infty} \beta_n^{(\ell)}(0) E^n}. \tag{80}$$

Using equation (3.6.22) of the book by Abramowitz *et al*,

$$\frac{a_0 + a_1 x + a_2 x^2 + \cdots}{b_0 + b_1 x + b_2 x^2 + \cdots} = \frac{a_0}{b_0} \left[1 + \left(\frac{a_1}{a_0} - \frac{b_1}{b_0}\right) x + \left(\frac{a_2}{a_0} - \frac{b_1(a_1 b_0 - a_0 b_1)}{a_0 b_0^2} - \frac{b_2}{b_0}\right) x^2 + \cdots\right],$$

the division of two polynomials in equation (80) is done as follows:

$$k^{2\lambda+1} [\cot \delta_\ell(E) - h(k)] = -\frac{1}{a^{(\ell)}} + \frac{r_0^{(\ell)}}{2} k^2 + \cdots, \tag{81}$$

where the scattering length $a^{(\ell)}$ and the effective radius $r_0^{(\ell)}$ for the state with the angular momentum ℓ are given by

$$a^{(\ell)} = -\frac{\beta_0^{(\ell)}}{\alpha_0^{(\ell)}}, \tag{82}$$

$$r_0^{(\ell)} = \frac{\hbar^2}{\mu} \left(\frac{\alpha_1^{(\ell)}}{\beta_0^{(\ell)}} - \frac{\alpha_0^{(\ell)} \beta_1^{(\ell)}}{\beta_0^{(\ell)2}}\right). \tag{83}$$

9. A numerical example related to quantum dot theory

To demonstrate how the proposed method works, we use the following circularly symmetric potential, which is motivated by the models that are currently used in the theory of quantum dots,

$$U(r) = V_0 (r - r_0)\, \mathrm{e}^{-r/R}, \tag{84}$$

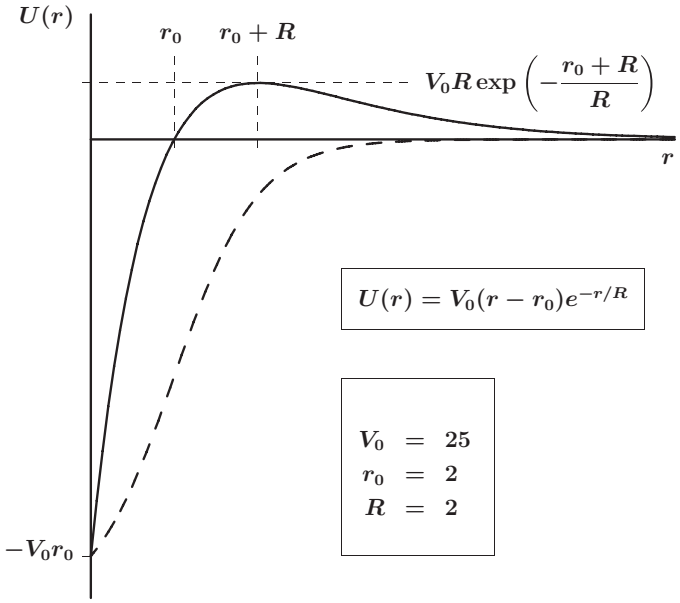

Figure 3. Model potential (84) measured in the donor Hartree units 10.96 meV as a function of the distance measured in the units of donor Bohr radius 101.89 Å. The dashed curve is a typical potential for an empty 2D quantum dot.

with $V_0 = 25$, $r_0 = 2$ and $R = 2$, where V_0 (as well as all the energies in this example) is measured in the so-called donor Hartree units and the distances in the units of 'donor Bohr radius', which were chosen to be 10.96 meV and 101.89 Å, respectively. These values for the units are relevant to the motion of electrons in the semiconductor material GaAs [28], where the effective electron mass is $\mu = 0.063m_e$ (with m_e being free electron mass).

Although strictly the potential (84) should be considered as an abstract quantum-mechanical 'toy' model, we chose its shape in such a way that it resembles the potentials that are currently used to describe the 2D quantum dots (see, for example, [28–31]). As is seen in figure 3, our potential has a repulsive barrier which is not present in the traditional quantum dot models. The main reason for introducing such a barrier was to enrich our 'toy' model spectrum with resonances. However, one can argue that such a barrier may appear in real quantum dots as well. Indeed, when electrons fill up the lower levels of a dot, they should repel each other and tend to stay mostly at its periphery. This means that for an additional incoming electron, the attractive force at the center is reduced and a repulsion appears at the border. In other words, the original empty-dot confining potential (shown with the dashed curve) is transformed into something that looks like our 'toy' potential. Of course, this speculative reasoning does not mean that we claim that our potential is something more than an abstract model.

Since nothing special is associated with the angular momentum, we only consider here the S-wave states ($\ell = 0$). For such a case, the potential (84) supports three bound states and a sequence of resonances. These spectral points (given in table 1 and shown in figure 3) were located using the exact approach, i.e. as the roots of equation (9), where $f_\ell^{(\mathrm{in})}$ is the asymptotic value (11) of the solution of equation (14).

To make sure that we did not miss any of the bound states and/or narrow resonances, we calculated the S-wave scattering phase shift and checked if it obeys Levinson's theorem. In

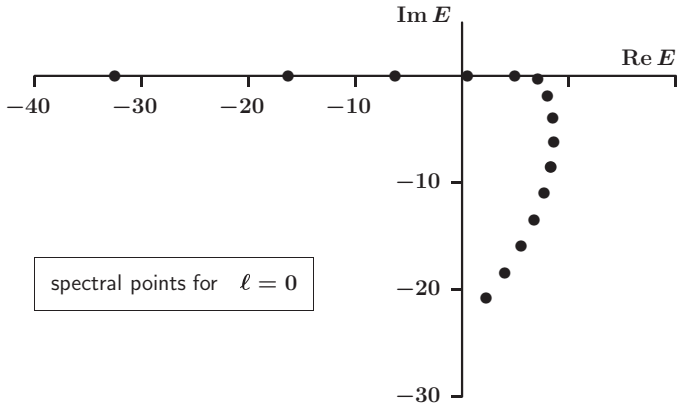

Figure 4. Spectral points generated by the potential (84). Their numerical values are given in table 1.

Table 1. Spectral points $E = E_r - \mathrm{i}\Gamma/2$ (in the units 10.96 meV) generated by the potential (84). Their distribution on the complex energy surface is shown in figure 4.

E_r	Γ
−32.485 042 8093	0
−16.264 365 0096	0
−6.271 150 4590	0
0.503 618 0960	2×10^{-15}
4.942 244 0057	0.000 058 8188
7.105 016 8573	0.571 077 6714
7.998 740 9699	3.668 497 7768
8.502 563 7363	7.760 574 3107
8.593 755 4145	12.305 258 1635
8.319 312 1385	17.092 263 8769
7.695 296 9586	21.966 391 6836
6.743 661 2278	26.936 755 5304
5.524 404 0747	31.868 859 1621
4.010 010 3640	36.811 885 3195
2.260 361 4329	41.649 028 4540

[9, 32, 33] it was shown that in the absence of a zero-energy bound state for the P-wave and always for the S-wave, this theorem is the same as for the 3D scattering, namely

$$\delta_\ell(0) - \delta_\ell(\infty) = \pi N_\ell, \tag{85}$$

where N_ℓ is the number of bound states with the angular momentum ℓ. If the energy moves to the right along the real axis, the phase shift increases by π near each resonance which is not far from the real axis. The smaller the width, the sharper the increase. When calculating the phase shift numerically, it is easy to miss a sharp jump corresponding a narrow resonance. Curve 'A' in figure 5 is an example of such omissions (the first two resonances are missed because of too large a step along the E-axis). The correct phase shift is shown by curve 'B'. It starts with 3π at the threshold and tends to zero at infinity, in accordance with equation (85).

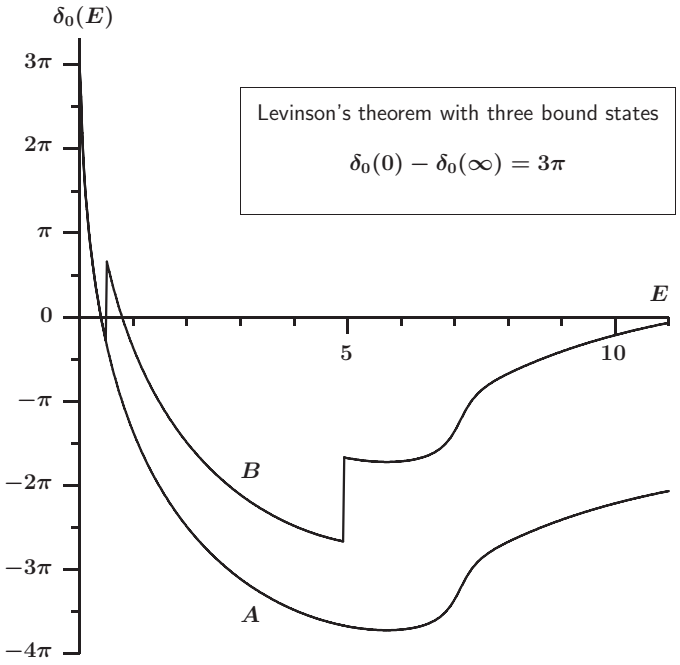

Figure 5. S-wave scattering phase shift for the potential (84). In curve 'A' the sharp jumps in π (corresponding to the first two extremely narrow resonances) are missing and as a result it does not obey Levinson's theorem.

Calculating the first two expansion coefficients and using equations (82) and (83), we found the following scattering length and effective radius:

$$a_0 = -0.452\,126\,0323 \text{ (dimensionless)}, \qquad r_0 = 0.058\,679\,0752 \text{ (length}^2\text{)}.$$

As a first test of expansions (69) and (70), we performed them at several scattering energies (i.e. on the real energy axis) and compared the approximate cross section obtained from the approximate Jost functions (see appendix A4) with the corresponding exact cross section that was calculated using the exact Jost functions via numerical integration of the system of differential equations (14) and (15). Figure 6 shows the exact cross section in the interval $E \in (0, 10]$ (thick curve) and the approximate cross sections (thin curves) when only the first five terms of the series (69), (70) were taken into account for E_0 being 1, 5 and 7. It is seen that within a rather wide interval around each E_0, the expansion reproduces the cross section very well even with all its zigzags.

The next step was to test our expansions at complex energies. To begin with, we performed them around a point on the real axis, namely around $E_0 = 7$ (far away from the threshold energy) and looked at the Jost function at the nearby complex energies. Why 7? Simply because there is a resonance not far from this point (third resonance of table 1). To check the accuracy of the expansion, we compared the approximate values of $f_\ell^{(\text{in})}(E)$ at various points around E_0 with the corresponding exact values of the Jost function. Apparently, the closer the point E is to the center of the expansion, the more accurate should be the result. Figure 7 shows three closed contours around $E_0 = 7$. Within the smallest of them the relative error of $f_\ell^{(\text{in})}(E)$ obtained by expansion (69) with $N = 4$ is less than 1%. The other two contours show the domains of 5% and 10% accuracy. The important fact is that even if the expansion is done

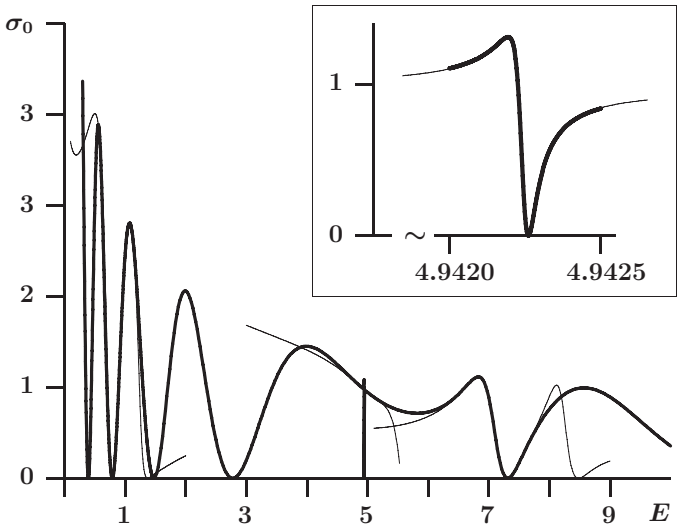

Figure 6. Comparison of the exact (thick curve) and approximate (thin curve) S-wave cross section for the potential (84). The approximate curves are obtained using expansion (69) with $N = 4$ (five terms) near the points $E_0 = 1 \times 10.96$ meV, $E_0 = 5 \times 10.96$ meV and $E_0 = 7 \times 10.96$ meV. The inset shows a magnified fragment of the curves near the second resonance.

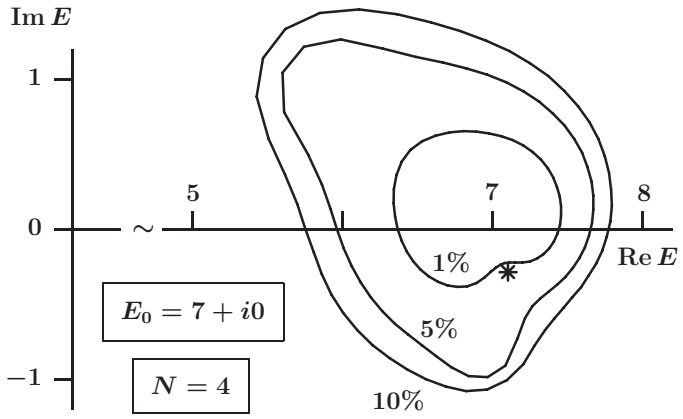

Figure 7. The domains within which the Jost function for the potential (84) is reproduced, using the first five terms ($N = 4$) of expansion (69), with the accuracy better than 1%, 5% and 10%. The expansion is done around the point $E_0 = 7 \times [10.96$ meV] on the real axis. The star shows the third resonance given in table 1.

on the real axis, the semi-analytic formulae (69) and (70) remain valid at the nearby complex points.

The star in figure 7 is a resonant zero of the exact Jost function. As is seen, the 1%-contour has a 'dent' near this point. The reason for it is that in calculating the relative error, we have an exact value of $f_\ell^{(\mathrm{in})}(E)$ in the denominator and this value is zero at the resonance. By the way, the approximate Jost function (69) with $N = 4$ has zero at $E = 7.105\,167\,9246 - \frac{\mathrm{i}}{2}0.568\,368\,5515$ which is not far from its exact position. This means that the expansion done on the real axis can be used for locating narrow resonances.

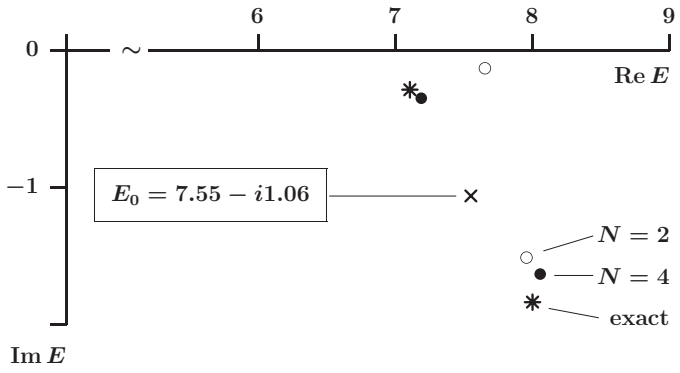

Figure 8. Spectral points corresponding to the third and fourth resonances of the potential (84). Stars show their exact locations. Open and filled circles are obtained using expansion (69) with $N = 2$ (three terms) and $N = 4$ (five terms), respectively. The expansion is done around the point $E_0 = (7.55 - \mathrm{i}1.06) \times 10.96$ meV, which is in the middle of these two resonances.

Finally, we tested the expansion around a point in the fourth quadrant (where the resonances are) of the complex energy plane. When solving the differential equations (65), (66); we used the complex rotation of the coordinate (see section 4) with such an angle θ that $\mathrm{Im}\,(k_0 r) = 0$ (where k_0 is the momentum corresponding to E_0). This guarantees that E_0 is within the domain $\mathcal{D}$ (see section 6).

Figure 8 shows the exact positions of two resonances (indicated with stars), the center of the expansion (cross) at $E_0 = 7.55 - \mathrm{i}1.06$, which is in the middle between them, and two pairs of the approximate locations of these resonances: open circles for three terms of the expansion and filled circles for five expansion terms. It is seen that the expansion converges, i.e. the more terms are taken into account, the more accurately the resonances are reproduced. It should be noted that the chosen position of E_0 is the 'worst case'. If we move E_0 a bit closer toward one of the resonances, it is reproduced much more accurately.

10. Conclusion

In this paper, we show that the Jost function for the two-dimensional scattering can be written as a sum of two terms, one of which is an analytic single-valued function of the energy E, while the other term can be factorized in an analytic function of E and a logarithmic function of the momentum. This means that the (logarithmic) branching point of the Riemann energy surface is given in the Jost function explicitly via the logarithmic factor. The remaining energy-dependent functions are defined on a single energy plane which no longer has any branching points. For these energy-dependent functions, we derive a system of first-order differential equations. Then, using the fact that the functions are analytic within a certain domain $\mathcal{D}$, we expand them in the power series around an arbitrary point $E_0 \in \mathcal{D}$ and obtain a system of differential equations that determine the expansion coefficients.

A systematic procedure developed in this paper allows us to accurately calculate the power series expansion of the Jost function practically at any point on the Riemann surface of the energy. Actually, the expansion is done for the single-valued functions of the energy, while the choice of the sheet of the Riemann surface is done by appropriately choosing the sheet of the logarithmic function of the momentum.

The method suggested in this paper makes it possible to obtain a semi-analytic expression for the two-dimensional Jost function (and therefore for the corresponding S-matrix) near an arbitrary point on the Riemann surface and thus to locate the resonant states as the S-matrix poles. Alternatively, the expansion can be used to parametrize experimental data, where the unknown expansion coefficients are the fitting parameters. Such a parametrization will have the correct analytic structure. After fitting the data given at real energies, one can use the semi-analytic Jost function to search for resonances in the nearby domain of the Riemann surface. The efficiency and accuracy of the suggested expansion are demonstrated by an example of a two-dimensional model potential.

In this paper, we restrict our consideration to a class of circularly symmetric short-range potentials (that vanish at infinity faster than any power of $1/r$). In principle, the theory should remain the same for any potential vanishing faster than the centrifugal term ($\sim 1/r^2$) of equation (4). In such a case this equation asymptotically behaves as equation (5) and therefore all our derivations remain valid. The only difficulty is that the analyticity domain $\mathcal{D}$ must be much more narrow than is given by condition (51) and shown in figure 2. Moreover, it is unclear how to obtain this condition for such a potential. This however does not mean that the theory is not applicable in such a case. Indeed, using the complex rotation, we can always extend $\mathcal{D}$ to practically whole E-plane no matter how narrow the initial $\mathcal{D}$ is.

As far as the potentials vanishing as $\sim 1/r^2$ or slower are concerned, our theory needs modification. In such a case, the asymptotic solutions of equation (4) are different from the Riccati–Bessel functions. In particular for a potential with Coulombic tails, the Riccati–Bessel and Riccati–Neumann functions should be replaced with the corresponding regular and irregular Coulomb functions that have much more complicated power series expansions.

The theory also needs modification for potentials that are not circularly symmetric. In such a case the angular momentum is not conserved and instead of a single radial equation (4), we have a set of coupled equations for different ℓ, which can be considered as a single matrix equation. The Jost function becomes a matrix as well as all the other quantities in the theory. Similarly, a matrix generalization of the proposed method is needed for multi-channel systems.

Acknowledgments

We gratefully acknowledge financial support from the National Research Foundation (NRF) of South Africa as well as from Swedish International Development Cooperation Agency (SIDA).

Appendix A. 2D partial-wave decomposition

The partial-wave decomposition of the wavefunction, scattering amplitude and cross section for a particle moving on a plane is done using the cylindrical coordinates where the z-axis (perpendicular to the plane) is needed to define the orbital angular momentum. All the steps of such a decomposition are similar to the 3D case, but the resulting formulae are not obvious and cannot be easily obtained from the corresponding 3D analysis. The derivations of various formulae of this type are given in several different papers (see, for example, [34, 35]). Usually, these derivations are very concise with many details omitted. Since such derivations are not present in the standard textbooks on quantum mechanics, we feel that it is worthwhile to collect everything in one place. This is why we include this appendix.

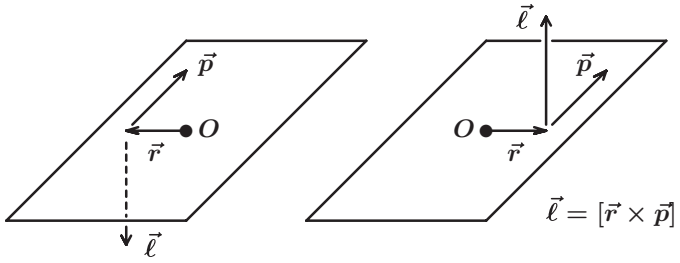

Figure 9. Two possible directions of the angular momentum for a particle moving on a plane.

A.1. Radial Schrödinger equation

Consider a particle of mass μ, moving on a plane and being affected by a force that is described by a potential $U(\vec{r})$, which is assumed to be of short range and circularly symmetric,

$$U(\vec{r}) = U(|\vec{r}|).$$

To make the derivations simple, we assume that our particle does not have spin (this restriction can be easily revoked later). In the coordinate representation, the Hamiltonian H of such a particle is most conveniently expressed using the polar coordinates

$$H = -\frac{\hbar^2}{2\mu}\Delta + U,$$

$$\Delta = \frac{1}{r}\frac{\partial}{\partial r}\left(r\frac{\partial}{\partial r}\right) + \frac{1}{\hbar^2 r^2}\hat{L}^2,$$

where

$$\hat{L}^2 = \hbar^2\frac{\partial^2}{\partial\varphi^2}$$

is the 2D operator of the square of the angular momentum. Its eigenfunctions $\mathcal{Y}_m(\varphi)$ obeying the equation

$$\hat{L}^2\mathcal{Y}_m(\varphi) = -\hbar^2 m^2\mathcal{Y}_m(\varphi)$$

and normalized as

$$\int_0^{2\pi}\mathcal{Y}_m^*(\varphi)\mathcal{Y}_{m'}(\varphi)\,\mathrm{d}\varphi = \delta_{mm'}, \tag{A.1}$$

are easy to find

$$\mathcal{Y}_m(\varphi) = \frac{1}{\sqrt{2\pi}}\,\mathrm{e}^{\mathrm{i}m\varphi}, \qquad m = 0, \pm1, \pm2, \ldots. \tag{A.2}$$

From the definition of the Fourier series on the interval $[0, 2\pi]$, it follows that

$$\sum_{m=-\infty}^{+\infty}\mathcal{Y}_m(\varphi)\mathcal{Y}_m^*(\varphi') = \delta(\varphi - \varphi'). \tag{A.3}$$

Each value of the angular momentum (except for zero) is represented twice: with two opposite signs. Classically, these two states correspond to the motion of the particle at the same distance r from the center and with the same velocity, but at different sides of the center (see figure 9).

The quantum number of the angular momentum $\ell = |m|$ is always non-negative and irrespective of its magnitude (if $\ell \neq 0$), the vector $\vec{\ell}$ can have two (only two) directions: up

or down (like the spin-1/2). The quantum number $m = \pm\ell$ is its z-component. In principle, we can use the same notation for the eigenfunctions of the operator $\hat{L}^2$ as in the 3D case, namely $\mathcal{Y}_{\ell m}$ with two subscripts. However, because of the relation $m = \pm\ell$, the subscript ℓ is redundant.

This can be formulated in a different way. The functions (A.2) form a complete orthonormal set on the interval $\varphi \in [0, 2\pi]$. This means that any (reasonable) function $f(\varphi)$ defined on this interval can be written as their linear combination, and such a combination can be written in the following two (equivalent) ways:

$$f(\varphi) = \sum_{m=-\infty}^{+\infty} a_m \mathcal{Y}_m(\varphi) = \sum_{\ell=0}^{\infty} \sum_{m=\pm\ell} \tilde{a}_{\ell m} \mathcal{Y}_m(\varphi), \qquad a_m = \tilde{a}_{|m|m}.$$

In other words, the following summations are equivalent:

$$\sum_{m=-\infty}^{+\infty} \longleftrightarrow \sum_{\ell=0}^{\infty} \sum_{m=\pm\ell}.$$

The operator corresponding to the quantum number m is obtained as follows. The gradient operator in the cylindrical coordinates is

$$\vec{\nabla} = \hat{\vec{r}} \frac{\partial}{\partial r} + \hat{\vec{\varphi}} \frac{1}{r} \frac{\partial}{\partial \varphi} + \hat{\vec{z}} \frac{\partial}{\partial z}, \tag{A.4}$$

where

$$\hat{\vec{r}} = [\hat{\vec{\varphi}} \times \hat{\vec{z}}], \qquad \hat{\vec{\varphi}} = [\hat{\vec{z}} \times \hat{\vec{r}}], \qquad \hat{\vec{z}} = [\hat{\vec{r}} \times \hat{\vec{\varphi}}]$$

are the corresponding unit vectors. Then

$$[\vec{r} \times \vec{p}] = r\hat{\vec{r}} \times \frac{\hbar}{\mathrm{i}} \vec{\nabla} = \frac{\hbar r}{\mathrm{i}} \left(\hat{\vec{z}} \frac{1}{r} \frac{\partial}{\partial \varphi} - \hat{\vec{\varphi}} \frac{\partial}{\partial z} \right)$$

and thus

$$\ell_z = \frac{\hbar}{\mathrm{i}} \frac{\partial}{\partial \varphi}.$$

Apparently, both $\hat{L}^2$ and ℓ_z commute with the Hamiltonian. The quantum numbers ℓ and m are therefore conserving. When specifying m, we implicitly specify the quantum number ℓ as well. This means that the quantum state of the particle is determined by two conserving quantum numbers, namely the energy E and the z-component of the angular momentum m. The corresponding wavefunction, obeying the Schrödinger equation,

$$H\psi_{\mathrm{Em}}(\vec{r}) = E\psi_{\mathrm{Em}}(\vec{r}),$$

can be factorized in the radial and angular parts

$$\psi_{\mathrm{Em}}(\vec{r}) = \frac{u_m(E, r)}{\sqrt{r}} \mathcal{Y}_m(\varphi), \tag{A.5}$$

where $\sqrt{r}$ in the denominator is introduced to obtain the radial equation without the first derivative. Substituting this factorized form into the Schrödinger equation, we obtain

$$\left[\frac{\mathrm{d}^2}{\mathrm{d}r^2} + k^2 - \frac{m^2 - 1/4}{r^2} - V(r) \right] u_m(E, r) = 0, \tag{A.6}$$

where k is the wave number (linear momentum) defined by

$$k^2 = \frac{2\mu}{\hbar^2} E \tag{A.7}$$

and $V(r)$ is the reduced (in the units of (length)$^{-2}$) potential

$$V(r) = \frac{2\mu}{\hbar^2}U(r).$$

Noting that equation (A.6) is exactly the same for both choices of the sign for m, we conclude that $u_m(E, r)$ actually depends on ℓ but not on m. The radial equation can therefore be re-written in the way we used to see it in the 3D problems

$$\left[\frac{\mathrm{d}^2}{\mathrm{d}r^2} + k^2 - \frac{\lambda(\lambda+1)}{r^2} - V(r)\right] u_\ell(E, r) = 0, \tag{A.8}$$

where we introduced

$$\lambda = \ell - \tfrac{1}{2} \tag{A.9}$$

and did the replacement

$$\ell^2 - \tfrac{1}{4} = \left(\ell - \tfrac{1}{2}\right)\left(\ell + \tfrac{1}{2}\right) = \lambda(\lambda+1).$$

Formally, equation (A.8) looks exactly like the radial equation of the 3D problem. The only difference is that λ is not an integer number

$$\lambda = -\tfrac{1}{2}, \tfrac{1}{2}, \tfrac{3}{2}, \tfrac{5}{2}, \ldots.$$

This simple fact makes a huge difference: it changes the analytic properties of the Jost function and thus the S-matrix, because the Riccati–Neumann function $y_\lambda(kr)$ with a half-integer λ has a logarithmic branching point on the Riemann surface of the energy [17].

A.2. Plane wave and circular waves

Consider a 2D plane wave normalized to the δ-function

$$\langle \vec{r}|\vec{k}\rangle = \frac{\mathrm{e}^{\mathrm{i}\vec{k}\vec{r}}}{2\pi}, \qquad \langle \vec{k}'|\vec{k}\rangle = \delta(\vec{k}' - \vec{k}) = \frac{1}{k}\delta(k'-k)\delta(\varphi'-\varphi), \tag{A.10}$$

where φ is the polar angle of the momentum $\hbar\vec{k}$. This plane wave can be expanded over the full set $\{\mathcal{Y}\}$ of the angular functions (A.2),

$$\frac{\mathrm{e}^{\mathrm{i}\vec{k}\vec{r}}}{2\pi} = \frac{\mathrm{e}^{\mathrm{i}kr\cos\varphi}}{2\pi} = \sum_{\ell m} a_m(kr)\mathcal{Y}_m(\varphi), \tag{A.11}$$

where the x-axis is directed along the coordinate vector $\vec{r}$. The expansion coefficients

$$a_m(kr) = \frac{1}{(2\pi)^{3/2}}\int_0^{2\pi} \mathrm{e}^{\mathrm{i}(kr\cos\varphi - m\varphi)}\,\mathrm{d}\varphi \tag{A.12}$$

can be found using the integral representation of the Bessel function [17]

$$\begin{aligned} J_m(z) &= \frac{1}{\pi\,\mathrm{i}^m}\int_0^{\pi} \mathrm{e}^{\mathrm{i}z\cos\varphi}\cos(m\varphi)\,\mathrm{d}\varphi = \frac{1}{2\pi\,\mathrm{i}^m}\int_0^{\pi} \mathrm{e}^{\mathrm{i}z\cos\varphi}(\mathrm{e}^{\mathrm{i}m\varphi} + \mathrm{e}^{-\mathrm{i}m\varphi})\,\mathrm{d}\varphi \\ &= \frac{1}{2\pi\,\mathrm{i}^m}\int_{-\pi}^{\pi} \mathrm{e}^{\mathrm{i}(z\cos\varphi - m\varphi)}\,\mathrm{d}\varphi = \frac{\mathrm{i}^m}{2\pi}\int_0^{2\pi} \mathrm{e}^{\mathrm{i}(-z\cos\varphi - m\varphi)}\,\mathrm{d}\varphi. \end{aligned} \tag{A.13}$$

Comparing equation (A.12) with (A.13) and using the symmetry property of the Bessel function $J_m(-z) = (-1)^m J_m(z)$, we see that

$$a_m(kr) = \frac{\mathrm{i}^m}{\sqrt{2\pi}}J_m(kr) \tag{A.14}$$

and thus

$$\frac{e^{i\vec{k}\vec{r}}}{2\pi} = \frac{1}{2\pi}\sum_{\ell m} i^m e^{im\varphi} J_m(kr) = \frac{1}{2\pi}\sum_{-\infty}^{+\infty} i^m e^{im\varphi} J_m(kr) = \frac{1}{\sqrt{2\pi}}\sum_{-\infty}^{+\infty} i^m J_m(kr)\mathcal{Y}_m(\varphi). \quad (A.15)$$

Using another symmetry property, $J_{-m}(z) = (-1)^m J_m(z)$, we see that the product $i^m J_m(kr)$ does not depend on the sign of m and thus this expansion can be re-written as

$$\frac{e^{i\vec{k}\vec{r}}}{2\pi} = \frac{1}{2\pi}\left[J_0(kr) + \sum_{\ell=1}^{\infty} i^\ell (e^{i\ell\varphi} + e^{-i\ell\varphi}) J_\ell(kr)\right]$$

$$= \frac{1}{2\pi}\sum_{\ell=0}^{\infty} \epsilon_\ell i^\ell \cos(\ell\varphi) J_\ell(kr), \quad (A.16)$$

where ϵ_ℓ is the 'multiplicity' of an ℓ-state, i.e. is the analogue of the factor $(2\ell+1)$ of the 3D case

$$\epsilon_\ell = \begin{cases} 1, & \ell = 0, \\ 2, & \ell > 0. \end{cases} \quad (A.17)$$

Expressing the Bessel function via the Riccati–Hankel functions

$$J_\ell(z) = \sqrt{\frac{1}{2\pi z}}\left[h^{(-)}_{\ell-1/2}(z) + h^{(+)}_{\ell-1/2}(z)\right],$$

we obtain the following decomposition of the 2D plane wave in the incoming $(-)$ and outgoing $(+)$ circular waves

$$\frac{e^{i\vec{k}\vec{r}}}{2\pi} = \frac{1}{2\pi\sqrt{kr}}\sum_{\ell=0}^{\infty}\sum_{m=\pm\ell} i^\ell\left[h^{(-)}_\lambda(kr) + h^{(+)}_\lambda(kr)\right]\mathcal{Y}_m(\varphi), \quad (A.18)$$

where λ is defined by equation (A.9).

In the above, we assumed that vector $\vec{r}$ was directed along the x-axis. If this is not the case, then the dot product

$$\vec{k}\vec{r} = kr(\cos\varphi_k\cos\varphi_r + \sin\varphi_k\sin\varphi_r) = kr\cos(\varphi_r - \varphi_k)$$

depends on the two polar angles. In this general case the plane wave is expanded over two sets of functions $\{\mathcal{Y}(\varphi_k)\}$ and $\{\mathcal{Y}(\varphi_r)\}$ depending on the angles of the momentum and coordinate vectors. In a similar way, as we did it above, it is not difficult to show that

$$\frac{e^{i\vec{k}\vec{r}}}{2\pi} = \sum_{-\infty}^{+\infty} i^m J_m(kr)\mathcal{Y}^*_m(\varphi_r)\mathcal{Y}_m(\varphi_k) = \sum_{\ell=0}^{\infty} i^\ell J_\ell(kr)\sum_{m=\pm\ell}\mathcal{Y}^*_m(\varphi_r)\mathcal{Y}_m(\varphi_k)$$

$$= \frac{1}{2\pi}\sum_{\ell=0}^{\infty}\epsilon_\ell i^\ell\cos\left[\ell(\varphi_r - \varphi_k)\right]J_\ell(kr)$$

$$= \frac{1}{\sqrt{2\pi kr}}\sum_{\ell m} i^\ell\left[h^{(-)}_\lambda(kr) + h^{(+)}_\lambda(kr)\right]\mathcal{Y}^*_m(\varphi_r)\mathcal{Y}_m(\varphi_k)$$

$$= \frac{1}{\sqrt{2\pi kr}}\sum_{\ell m} i^\ell u^{(0)}_\ell(E, r)\mathcal{Y}^*_m(\varphi_r)\mathcal{Y}_m(\varphi_k), \quad (A.19)$$

where

$$u^{(0)}_\ell(E, r) = h^{(-)}_\lambda(kr) + h^{(+)}_\lambda(kr) = 2j_\lambda(kr) \quad (A.20)$$

is a regular solution of the radial Schrödinger equation (A.8) for the case $V(r) \equiv 0$. These partial-wave decompositions can be conveniently written in the following symbolic form:

$$|\vec{k}\rangle = \sum_{\ell m} |k\ell m\rangle \mathcal{Y}_m(\varphi_k), \qquad |\vec{r}\rangle = \sum_{\ell m} |r\ell m\rangle \mathcal{Y}_m(\varphi_r), \tag{A.21}$$

$$\langle r\ell m|k\ell' m'\rangle = \delta_{\ell\ell'}\delta_{mm'} \mathrm{i}^\ell J_\ell(kr) = \delta_{\ell\ell'}\delta_{mm'} \mathrm{i}^\ell \sqrt{\frac{2}{\pi kr}}\, j_\lambda(kr), \tag{A.22}$$

$$\langle \vec{r}|k\ell m\rangle = \mathrm{i}^\ell \sqrt{\frac{2}{\pi kr}}\, j_\lambda(kr) \mathcal{Y}^*_m(\varphi_r), \qquad \langle \vec{k}|r\ell m\rangle = (-\mathrm{i})^\ell \sqrt{\frac{2}{\pi kr}}\, j_\lambda(kr) \mathcal{Y}^*_m(\varphi_k), \tag{A.23}$$

$$\langle k\ell m|k'\ell' m'\rangle = \frac{1}{k}\delta(k-k')\delta_{\ell\ell'}\delta_{mm'}, \qquad \langle r\ell m|r'\ell' m'\rangle = \frac{1}{r}\delta(r-r')\delta_{\ell\ell'}\delta_{mm'}, \tag{A.24}$$

$$\int_0^\infty \sum_{\ell m} |k\ell m\rangle\langle k\ell m| k\,\mathrm{d}k = 1, \qquad \int_0^\infty \sum_{\ell m} |r\ell m\rangle\langle r\ell m| r\,\mathrm{d}r = 1. \tag{A.25}$$

A.3. Scattering wavefunction

The plane wave (A.19) is a scattering wavefunction $\psi_{\vec{k}}(\vec{r})$ for the particular case of $V(r) \equiv 0$. Apparently, the structure of its partial-wave decomposition should be the same for all potentials

$$\psi_{\vec{k}}(\vec{r}) = \frac{N}{\sqrt{2\pi kr}} \sum_{\ell m} \mathrm{i}^\ell u_\ell(E,r) \mathcal{Y}^*_m(\varphi_r) \mathcal{Y}_m(\varphi_k),$$

where the factor N is determined by the choice of the potential and the collision energy (for the free motion, $N = 1$ at all energies). The purpose of this factor is to always have exactly the same normalization, namely

$$\langle \psi_{\vec{k}}|\psi_{\vec{k}'}\rangle = \delta(\vec{k} - \vec{k}'). \tag{A.26}$$

An appropriate value for N can be found as follows. The Riccati–Hankel functions $h^{(\pm)}_\lambda(kr)$ are two linearly independent solutions of the radial Schrödinger equation (A.8) without the potential term. This means that for a short-range potential, its solution asymptotically behaves as a linear combination of the Riccati–Hankel functions

$$u_\ell(E,r) \underset{r\to\infty}{\longrightarrow} f^{(\mathrm{in})}_\ell(E) h^{(-)}_\lambda(kr) + f^{(\mathrm{out})}_\ell(E) h^{(+)}_\lambda(kr), \tag{A.27}$$

where the combination coefficients depend on the energy and are called the Jost functions. In fact, they are the amplitudes of the incoming $(-)$ and outgoing $(+)$ circular waves. On the other hand, at large distances the wavefunction $\psi_{\vec{k}}(\vec{r})$ consists of two parts: the initial (incident) wave $\psi^{(0)}_{\vec{k}}(\vec{r})$ and a scattered circular wave that goes in all directions with a certain amplitude F,

$$\psi_{\vec{k}}(\vec{r}) \underset{r\to\infty}{\longrightarrow} \psi^{(0)}_{\vec{k}}(\vec{r}) + F(E,\varphi_k,\varphi_r)\frac{\mathrm{e}^{\mathrm{i}kr}}{\sqrt{r}}.$$

If $\psi_{\vec{k}}(\vec{r})$ is properly normalized, then $\psi^{(0)}_{\vec{k}}(\vec{r}) \equiv \mathrm{e}^{\mathrm{i}\vec{k}\vec{r}}/(2\pi)$. This means that the radial wavefunction at large distances should also be split in two parts one of which coincides with function (A.20). In doing such a splitting of the function (A.27), we obtain

$$u_\ell(E,r) \underset{r\to\infty}{\longrightarrow} f^{(\mathrm{in})}_\ell \left[h^{(-)}_\lambda + h^{(+)}_\lambda + \left(\frac{f^{(\mathrm{out})}_\ell}{f^{(\mathrm{in})}_\ell} - 1 \right) h^{(+)}_\lambda \right]$$

and see that $N = 1/f^{(\mathrm{in})}_\ell$, i.e.

$$\psi_{\vec{k}}(\vec{r}) = \frac{1}{\sqrt{2\pi kr} f^{(\mathrm{in})}_\ell(E)} \sum_{\ell m} \mathrm{i}^\ell u_\ell(E,r) \mathcal{Y}^*_m(\varphi_r) \mathcal{Y}_m(\varphi_k). \tag{A.28}$$

A.4. Cross section

Defining the partial-wave S-matrix and the amplitude,

$$s_\ell(E) = \frac{f_\ell^{(\mathrm{out})}(E)}{f_\ell^{(\mathrm{in})}(E)}, \qquad f_\ell(E) = \frac{s_\ell(E) - 1}{\sqrt{2\pi \mathrm{i} k}},$$

and using

$$h_\lambda^{(+)}(kr) \underset{r\to\infty}{\longrightarrow} -\mathrm{i}\exp\left[\mathrm{i}(kr - \lambda\pi/2)\right],$$

as well as the fact that

$$\sum_m \mathcal{Y}_m^*(\varphi_r)\mathcal{Y}_m(\varphi_k) = \begin{cases} \dfrac{1}{2\pi}, & \ell = 0 \\ \dfrac{1}{2\pi}(\mathrm{e}^{-\mathrm{i}\ell\varphi_r}\,\mathrm{e}^{\mathrm{i}\ell\varphi_k} + \mathrm{e}^{\mathrm{i}\ell\varphi_r}\,\mathrm{e}^{-\mathrm{i}\ell\varphi_k}), & \ell > 0 \end{cases}$$
$$= \frac{\epsilon_\ell}{2\pi}\cos[\ell(\varphi_k - \varphi_r)],$$

we can write the asymptotic behavior of the scattering wavefunction as

$$\psi_{\vec{k}}(\vec{r}) \underset{r\to\infty}{\longrightarrow} \frac{1}{2\pi}\left[\mathrm{e}^{\mathrm{i}\vec{k}\vec{r}} + \mathcal{F}(E,\varphi)\frac{\mathrm{e}^{\mathrm{i}kr}}{\sqrt{r}}\right], \tag{A.29}$$

where $\varphi = \varphi_k - \varphi_r$ is the scattering angle and the total scattering amplitude has the following partial-wave expansion:

$$\mathcal{F}(E,\varphi) = \sum_{\ell=0}^{\infty} \epsilon_\ell f_\ell(E)\cos(\ell\varphi). \tag{A.30}$$

The cross section for a 2D scattering has the units of length. The number of particles scattered into the angle spanned by the arc $r\,\mathrm{d}\varphi$ is the product of the flux in that radial direction and the length of the arc. The corresponding cross section $\mathrm{d}\sigma$ is defined as such a length that after its multiplication by the total incoming flux, it gives the same number of particles, i.e.

$$|\vec{j}^{(\mathrm{in})}|\,\mathrm{d}\sigma = j_r^{(\mathrm{out})}(\varphi) r\,\mathrm{d}\varphi.$$

Using the standard definition for the particle flux $\vec{j} = \hbar/(2\mathrm{i}\mu)(\psi^*\vec{\nabla}\psi - \psi\vec{\nabla}\psi^*)$ with the operator $\vec{\nabla}$ given by equation (A.4), it is not difficult to find that the incoming (corresponding to the first term of wavefunction (A.29)) and outgoing (obtained from the second term of the same wavefunction) fluxes are

$$\vec{j}^{(\mathrm{in})} = \frac{\hbar\vec{k}}{(2\pi)^2\mu}, \qquad j_r^{(\mathrm{out})}(\varphi) = \frac{\hbar k\,|\mathcal{F}(E,\varphi)|^2}{(2\pi)^2\mu r}$$

and thus the differential cross section is

$$\frac{\mathrm{d}\sigma}{\mathrm{d}\varphi} = |\mathcal{F}(E,\varphi)|^2.$$

Using the integral

$$\int_0^{2\pi} \cos(\ell\varphi)\cos(\ell'\varphi)\mathrm{d}\varphi = \left\{\begin{matrix} 0, & \ell \neq \ell' \\ 2\pi, & \ell = \ell' = 0 \\ \pi, & \ell = \ell' \neq 0 \end{matrix}\right\} = \frac{2\pi}{\epsilon_\ell}\delta_{\ell\ell'}$$

the total cross section can be written as follows:

$$\sigma = \int_0^{2\pi} |\mathcal{F}(E,\varphi)|^2\,\mathrm{d}\varphi = \sum_\ell \sigma_\ell,$$
$$\sigma_\ell = 2\pi\epsilon_\ell\,|f_\ell(E)|^2 = \frac{\epsilon_\ell}{k}\,|s_\ell(E) - 1|^2\,, \tag{A.31}$$

where σ_ℓ is the partial-wave cross section.

Appendix B. Expansion coefficients for the holomorphic parts of the Riccati–Bessel and Riccati–Neumann functions

The Riccati–Bessel and Riccati–Neumann functions $j_\lambda(kr)$ and $y_\lambda(kr)$ can be written in the following factorized form:

$$j_\lambda(kr) = k^{\lambda+1}\tilde{j}_\lambda(E,r), \tag{B.1}$$

$$y_\lambda(kr) = k^{-\lambda}\tilde{y}_\lambda(E,r) + k^{\lambda+1}h(k)\tilde{j}_\lambda(E,r), \tag{B.2}$$

where the 'tilded' functions are holomorphic with respect to the energy variable E. This means that we can expand them in the Taylor series

$$\tilde{j}_\lambda(E,r) = \sum_{n=0}^{\infty} s_n^{(\lambda)}(E_0,r)\,(E-E_0)^n\,, \tag{B.3}$$

$$\tilde{y}_\lambda(E,r) = \sum_{n=0}^{\infty} c_n^{(\lambda)}(E_0,r)\,(E-E_0)^n\,, \tag{B.4}$$

near an arbitrary point E_0. The expansion coefficients,

$$s_n^{(\lambda)}(E_0,r) = \left.\frac{1}{n!}\frac{\partial^n}{\partial E^n}\tilde{j}_\lambda(E,r)\right|_{E=E_0}, \tag{B.5}$$

$$c_n^{(\lambda)}(E_0,r) = \left.\frac{1}{n!}\frac{\partial^n}{\partial E^n}\tilde{y}_\lambda(E,r)\right|_{E=E_0}, \tag{B.6}$$

are expressed via the corresponding derivatives. In order to find them, we note that

$$E = \frac{\hbar^2k^2}{2\mu} \quad\Longrightarrow\quad \frac{\partial}{\partial E} = \frac{\mu}{\hbar^2 k}\frac{\partial}{\partial k} \tag{B.7}$$

and also make use of the relations (which follow from equation (9.1.30) of the handbook by Abramowitz and Stegun [17])

$$\frac{\mathrm{d}}{\mathrm{d}z}\left[\frac{\mathcal{J}_\lambda(z)}{z^{\lambda+1}}\right] = -\frac{\mathcal{J}_{\lambda+1}(z)}{z^{\lambda+1}}, \tag{B.8}$$

$$\frac{\mathrm{d}}{\mathrm{d}z}[z^\lambda\mathcal{J}_\lambda(z)] = z^\lambda\mathcal{J}_{\lambda-1}(z), \tag{B.9}$$

where $\mathcal{J}_\lambda(z)$ stands for either $j_\lambda(z)$ or $y_\lambda(z)$. Therefore,

$$\frac{\partial}{\partial E}\tilde{j}_\lambda(E,r) = \frac{\mu}{\hbar^2k}\cdot\frac{\partial}{\partial k}\left[\frac{j_\lambda(kr)}{k^{\lambda+1}}\right] = \frac{\mu r^{\lambda+2}}{\hbar^2k}\cdot\frac{\partial}{\partial(kr)}\left[\frac{j_\lambda(kr)}{(kr)^{\lambda+1}}\right]$$

$$= -\frac{\mu r^{\lambda+2}}{\hbar^2k}\frac{j_{\lambda+1}(kr)}{(kr)^{\lambda+1}} = -\frac{\mu r}{\hbar^2}\tilde{j}_{\lambda+1}(E,r)$$

and thus

$$\frac{\partial^n}{\partial E^n}\tilde{j}_\lambda(E,r) = \left(-\frac{\mu r}{\hbar^2}\right)^n\tilde{j}_{\lambda+n}(E,r), \tag{B.10}$$

$$s_n^{(\lambda)}(E_0,r) = \frac{1}{n!}\left(-\frac{\mu r}{\hbar^2}\right)^n\left[\frac{j_{\lambda+n}(kr)}{k^{\lambda+n+1}}\right]_{E=E_0} = \frac{1}{n!}\left(-\frac{\mu r}{\hbar^2}\right)^n\sqrt{\frac{\pi r}{2}}\left[\frac{J_{\ell+n}(kr)}{k^{\ell+n}}\right]_{E=E_0}. \tag{B.11}$$

As it should be (since $\tilde{j}_\lambda(E,r)$ is single valued), the expansion coefficients $s_n^{(\lambda)}(E_0,r)$ do not depend on the choice of the sign of the momentum $k_0=\pm\sqrt{2\mu E_0/\hbar^2}$. Indeed,

$$\frac{j_{\lambda+n}(kr)}{k^{\lambda+n+1}}=\sqrt{\frac{\pi kr}{2}}\frac{J_{\lambda+n+1/2}(kr)}{k^{\lambda+n+1}}=\sqrt{\frac{\pi r}{2}}\frac{J_{\lambda+n+1/2}(kr)}{k^{\lambda+n+1/2}}, \tag{B.12}$$

and since (see equation (9.1.35) of [17])

$$J_\nu(z\,\mathrm{e}^{\mathrm{i}\pi})=(\mathrm{e}^{\mathrm{i}\pi})^\nu J_\nu(z), \tag{B.13}$$

the numerator and denominator in equation (B.12) acquire the same phase factor when k changes its sign.

Finding the derivative $\partial_E^n\tilde{y}_\lambda(E,r)$ is a little bit more complicated. The first derivative can be written as

$$\frac{\partial}{\partial E}\tilde{y}_\lambda(E,r)=\frac{\mu r^{1-\lambda}}{\hbar^2 k}\left\{\frac{\partial}{\partial(kr)}[(kr)^\lambda y_\lambda(kr)]-\frac{\partial}{\partial(kr)}[h(k)(kr)^\lambda j_\lambda(kr)]\right\}.$$

Using equation (B.9) and explicit form of the function $h(k)$ given by equation (31), we obtain

$$\begin{aligned}\frac{\partial}{\partial E}\tilde{y}_\lambda(E,r)&=\frac{\mu r^{1-\lambda}}{\hbar^2 k}\left[(kr)^\lambda y_{\lambda-1}(kr)-h(k)(kr)^\lambda j_{\lambda-1}(kr)-(kr)^\lambda j_\lambda(kr)\frac{2}{\pi kr}\right]\\&=\frac{\mu r}{\hbar^2}\left[k^{\lambda-1}y_{\lambda-1}(kr)-k^{\lambda-1}h(k)j_{\lambda-1}(kr)-\frac{2}{\pi r}k^{\lambda-2}j_\lambda(kr)\right]\\&=\frac{\mu r}{\hbar^2}\tilde{y}_{\lambda-1}(E,r)-\frac{2\mu}{\pi\hbar^2}k^{\lambda-2}j_\lambda(kr)\\&=\frac{\mu r}{\hbar^2}\tilde{y}_{\lambda-1}(E,r)-\frac{2\mu}{\pi\hbar^2}f_{\lambda1}(kr),\end{aligned} \tag{B.14}$$

where we introduced an auxiliary function

$$f_{\lambda n}(k,r)=k^{\lambda-2n}j_\lambda(kr)=k^{\ell-2n}\sqrt{\frac{\pi r}{2}}J_\ell(kr), \tag{B.15}$$

whose derivatives can be found using the following recurrence relation:

$$\begin{aligned}\frac{\partial}{\partial E}[k^{\lambda-2n}j_\lambda(kr)]&=\frac{\mu}{\hbar^2 k}r^{2n-\lambda+1}\frac{\partial}{\partial(kr)}\left[\frac{1}{(kr)^{2n}}(kr)^\lambda j_\lambda(kr)\right]\\&=\frac{\mu}{\hbar^2 k}r^{2n-\lambda+1}\left[-\frac{2n}{(kr)^{2n+1}}(kr)^\lambda j_\lambda(kr)+\frac{1}{(kr)^{2n}}(kr)^\lambda j_{\lambda-1}(kr)\right]\\&=-\frac{2n\mu}{\hbar^2}k^{\lambda-2(n+1)}j_\lambda(kr)+\frac{\mu r}{\hbar^2}k^{\lambda-1-2n}j_{\lambda-1}(kr),\end{aligned}$$

i.e.

$$\frac{\partial}{\partial E}f_{\lambda n}=-\frac{2n\mu}{\hbar^2}f_{\lambda,n+1}+\frac{\mu r}{\hbar^2}f_{\lambda-1,n}. \tag{B.16}$$

Repeatedly using relations (B.14) and (B.16), we can calculate any number of the derivatives $\partial_E^n\tilde{y}_\lambda(E,r)$ needed for finding the expansion coefficients (B.6).

References

[1] Aringazin A K, Dahnovsky Y, Krevchik V D, Semenov M B, Ovchinnikov A A and Yamamoto K 2003 Two-dimensional tunnel correlations with dissipation *Phys. Rev.* B **68** 155426

[2] Rakityansky S A 2003 Unified treatment of bound, scattering, and resonant states in one-dimensional semiconductor nanostructures *Phys. Rev.* B **68** 195320

[3] Rakityansky S A 2004 Modified transfer matrix for nanostructures with arbitrary potential profile *Phys. Rev.* B **70** 205323

[4] Bollé D and Gesztesy F 1984 Low-energy parametrization of scattering observables in n-dimensional quantum systems *Phys. Rev. Lett.* **52** 1469
[5] Bollé D and Gesztesy F 1984 Scattering observables in arbitrary dimension $n \geqslant 2$ *Phys. Rev.* A **30** 1279
[6] Verhaar B J, van den Eijnde J P H W, Voermans M A J and Schaffrath M M J 1984 Scattering length and effective range in two dimensions; application to adsorbed hydrogen atoms *J. Phys. A: Math. Gen.* **17** 595
[7] Verhaar B J, De Goey L P H, Vredenbregt E J D and van den Eijnde J P H W 1985 Scattering length and effective range for scattering in a plane and in higher dimensions *Phys. Lett.* A **110** 371
[8] Verhaar B J, De Goey L P H, Vredenbregt E J D and van den Eijnde J P H W 1985 Scattering length and effective range for scattering in a plane and in higher dimensions *Phys. Rev.* A **32** 1424
[9] Gibson W G 1986 Two-dimensional scattering: low-energy behaviour of the Jost function and Levinson's theorem *Phys. Lett.* A **117** 107
[10] Klawunn M, Pikovski A and Santos L 2010 Two-dimensional scattering and bound states of polar molecules in bilayers *Phys. Rev.* A **82** 044701
[11] Bethe H A 1949 Theory of the effective range in nuclear scattering *Phys. Rev.* **76** 38-50
[12] Helfrich K and Hammer H-W 2011 Resonant three-body physics in two spatial dimensions arXiv:1101.1891v1 [cond-mat.quant-gas]
[13] Rakityansky S A and Elander N 2009 Generalized effective-range expansion *J. Phys. A: Math. Theor.* **42** 225302
[14] Rakityansky S A and Elander N 2011 Multi-channel analog of the effective-range expansion *J. Phys. A: Math. Theor.* **44** 115303
[15] Brand L 1966 *Differential and Difference Equations* (New York: Wiley)
[16] Mathews J and Walker L R 1964 *Mathematical Methods of Physics* (New York: Benjamin)
[17] Abramowitz M and Stegun A (ed) 1964 *Handbook of Mathematical Functions* (Washington, DC: National Bureau of Standards)
[18] Rakityansky S A, Sofianos S A and Amos K 1996 A method of calculating the Jost function for analytic potentials *Nuovo Cimento* B **111** 363–78
[19] Sofianos S A and Rakityansky S A 1997 Exact method for locating potential resonances and Regge trajectories *J. Phys. A: Math. Gen.* **30** 3725
[20] Sofianos S A, Rakityansky S A and Vermaak G P 1997 Sub-threshold resonances in few-neutron systems *J. Phys. G: Nucl. Part. Phys.* **23** 1619–29
[21] Rakityansky S A and Sofianos S A 1998 Jost function for coupled partial waves *J. Phys. A: Math. Gen.* **31** 5149–75
[22] Sofianos S A, Rakityansky S A and Massen S E 1999 Jost function for singular potentials *Phys. Rev.* A **60** 337–43
[23] Rakityansky S A and Sofianos S A 1999 Jost function for coupled channels *Few-Body Syst. Suppl.* **10** 93–6
[24] Massen S E, Sofianos S A, Rakityansky S A and Oryu S 1999 Resonances and off-shell characteristics of effective interactions *Nucl. Phys.* A **654** 597–611
[25] Rakityansky S A, Sofianos S A and Elander N 2007 Padé approximation of the S-matrix as a way of locating quantum resonances and bound states *J. Phys. A: Math. Theor.* **40** 14857–69
[26] Poincaré H 1884 Sur les groupes des équations linéaires *Acta Math.* **4** 201–311
Lefschetz S 1957 *Differential Equations: Geometric Theory* (New York: Interscience)
[27] Motovilov A K 1993 *Theor. Math. Phys.* **95** 692
[28] Markvoort A J, Hilbers P A and Pino R 2003 Laterally coupled jellium-like two-dimensional quantum dots *J. Phys.: Condens. Matter* **15** 6977
[29] De Filippo S and Salerno M 2000 Spectral properties of a model potential for quantum dots with smooth boundaries *Phys. Rev.* B **62** 4230
[30] Adamowski J, Sobkowicz M, Szafran B and Bednarek S 2000 Electron pair in a Gaussian confining potential *Phys. Rev.* B **62** 4234
[31] Ciftja O 2007 An experimentally justified confining potential for electrons in two-dimensional semiconductor quantum dots *J. Comput.-Aided Mater. Des.* **14** 37
[32] Cheney M 1984 Two-dimensional scattering: the number of bound states from scattering data *J. Math. Phys.* **25** 1449–55
[33] Bollé D, Gesztesy F, Danneels C and Wilk S F J 1986 Threshold behavior and Levinson's theorem for two-dimensional scattering systems: a surprise *Phys. Rev. Lett.* **56** 900–3
[34] Lapidus I R 1982 Quantum-mechanical scattering in two dimensions *Am. J. Phys.* **50** 45
[35] Adhikari S K 1986 Quantum scattering in two dimensions *Am. J. Phys.* **54** 362